Geomechanics and Engineering, Vol. 1, No. 2 (2009) 113-120
DOI: http://dx.doi.org/10.12989/gae.2009.1.2.113

Shape factor s_γ for shallow footings

Viktor Puzakov†

Department of Civil Engineering, University of Minnesota, Minneapolis, MN 55455, U.S.A.

Andrew Drescher‡

Department of Civil Engineering, University of Minnesota, 500 Pillsbury, Minneapolis, MN 55455, U.S.A.

Radoslaw L. Michalowski‡†

Department of Civil and Environmental Engineering, University of Michigan, MI 48109, U.S.A.

(Received December 18, 2008, Accepted April 23, 2009)

Abstract. The results of *FLAC3D*-based numerical evaluation of the bearing capacity shape factor s_γ are presented for square and rectangular footings on granular soils. The results confirm a peculiar effect found earlier by Zhu and Michalowski (2005), where for large values of internal friction angle, s_γ exhibits a peak at some aspect ratio of the footing, and then decreases towards unity at large aspect ratios. The Zhu and Michalowski's results were derived using the finite element program *ABAQUS*, and the results presented in this note corroborate their earlier findings.

Keywords: footings; bearing capacity; shape factors; finite element method; three-dimensional analysis; numerical methods.

1. Introduction

There is a considerable body of literature regarding experimental and theoretical studies dedicated to the bearing capacities of square, rectangular, and circular shallow footings (Golder 1941, Meyerhof 1963, Hansen 1970, De Beer 1970, Bolton and Lau 1993, Michalowski 2001, Michalowski and Dawson 2002a, 2002b, Erickson and Drescher 2002, Lyamin *et al*. 2007). The results of these studies have been traditionally presented as shape factors (shape modifiers), denoted as s_c, s_q, and s_γ, used to modify strip footing bearing capacity factors, N_c, N_q and N_γ, in the formula for bearing capacity

$$p = cs_cN_c + qs_qN_q + 0.5\gamma Bs_\gamma N_\gamma \tag{1}$$

† Graduate Research Assistant
‡ Professor, E-mail: dresc001@umn.edu
‡† Professor, Corresponding author, E-mail: rlmich@umich.edu

where c is the cohesion of the soil, q is the surcharge, γ is the unit weight of the soil underneath the footing, and B is the width of the footing. Alternatively, formula (1) can be written as

$$p = cN_c^* + qN_q^* + 0.5\gamma BN_\gamma^* \tag{2}$$

where N_c^*, N_q^*, and N_γ^* are referred to as the modified bearing capacity factors. The shape factors can then be defined as

$$s_c = \frac{N_c^*}{N_c},\ s_q = \frac{N_q^*}{N_q},\ s_\gamma = \frac{N_\gamma^*}{N_\gamma} \tag{3}$$

Therefore, to determine shape factors s_c, s_q, and s_γ, for rectangular footings, the bearing capacity for such footings needs to be evaluated and compared with that of a strip footing.

In a recent paper by Zhu and Michalowski (2005), theoretical estimates of the shape factors for square and rectangular footings were obtained using numerical code *ABAQUS*, and the results were reported in tables and graphs. Using three-dimensional (brick) elements, footings with length/width aspect ratios, L/B, from 1 to 5 resting on weightless soil, or soil with weight, were considered for a range of friction angles ϕ from 0^o to 40^o. It was found that the dependence of shape factor s_γ on the internal friction angle and footing aspect ratio is rather complex. In particular, for friction angles less than 30^o, s_γ increases monotonically with the increase in L/B. On the other hand, for larger friction angle values, s_γ initially increases and then decreases with the increase in L/B; the latter implies the presence of a peak value of s_γ for some aspect ratio L/B. Zhu and Michalowski (2005) attributed this dependence to the effect of volumetric strain in plastically deforming material around the footing. Indeed, as the computations were performed assuming an elastic-perfectly plastic material model with the dilatancy angle equal to the friction angle, the larger the friction angle the more the material dilates, and the deforming zones along the footing width and length spread and interact in a complex fashion.

The focus of this study is factor s_γ, and not the remaining factors in Eq. (3). In particular, a peculiar effect will be investigated found earlier by Zhu and Michalowski (2005), where for large values of internal friction angle, s_γ exhibits a peak at some aspect ratio of the footing. We emphasize that the focus of this study is the unexpected shape of s_γ function, and not the numerical values of s_γ. The objective is to indicate whether the peculiarity (a peak) found in function s_γ might be an artifact of the method used, or is it an effect originating from the mechanics of the problem.

This note provides data on shape factor s_γ for square and rectangular footings obtained by means of *FLAC3D* (1997). A comparison of results obtained using different codes is of interest as there are conceptual and algorithmic differences between various codes. *ABAQUS* (standard) is an implicit code, whereas *FLAC3D* is an explicit (dynamic) code; also, the soil in *FLAC3D* is governed by the associative flow rule, whereas the plastic potential function in *ABAQUS* does not follow precisely the Mohr-Coulomb yield condition; rather, a smoothed approximation of the Mohr-Coulomb pyramid (albeit a very close one) is used to avoid numerical convergence problems. The reader will find the details of this model in Zhu and Michalowski (2005).

2. Simulations with *FLAC3D*

Numerical simulations of the bearing capacity were conducted for one-quarter of the footing and surrounding soil volume. Specifically, the soil volume ($20B \times 20B \times 10B$, B being the footing width) was discretized into 13,500 brick-type elements. This mesh is different from the one in Zhu and Michalowski (2005), who used the meshes from several hundred to 2,144 elements. However, the numbers of the elements used in the two analyses are not comparable directly, because the elements used by *FLAC3D* were 8-noded brick elements, whereas the elements generated by *ABAQUS* were 20-node elements.

The footing area in *FLAC3D* calculations was modeled with 100 equal size elements, and the outside volume was divided into elements gradually increasing in size, Fig. 1(a). Discretized models with several aspect ratios ranging from 1 to 4 were generated; additionally, a strip footing was modeled, where plane-strain conditions were enforced by the footing length extending to the side wall of the model. For comparison, simulations were performed using a bi-uniform mesh, in which constant size elements were used, Fig. 1(b). These resulted in higher bearing capacity estimates and they are not presented here. Kinematic boundary conditions allowing only vertical displacements were applied at the volume walls, and no-displacement boundary condition was enforced at the volume bottom.

The soil was modeled as elastic-perfectly plastic, obeying the flow rule associated with the Mohr-Coulomb yield condition. It is well established that limit loads calculated with non-associated flow rule cannot exceed those for associative rule (Radenkovic 1962). The use of the normality rule is made here to allow direct comparison of the results to other solutions available in the literature. The range of the friction angle used in these simulations spanned 15° to 40°. The Young's modulus ($E = 2 \times 10^8$ Pa) and Poisson's ratio ($\nu = 0.44$) selected for calculations assured that plastic yielding did not occur in simulations of the geostatic state of stress, which may happen when using a cohesionless yield condition. The bearing capacity of footings in simulations with elastic-perfectly plastic soil model is independent of the elastic modulus; indeed, a ten-fold reduction in the Young's

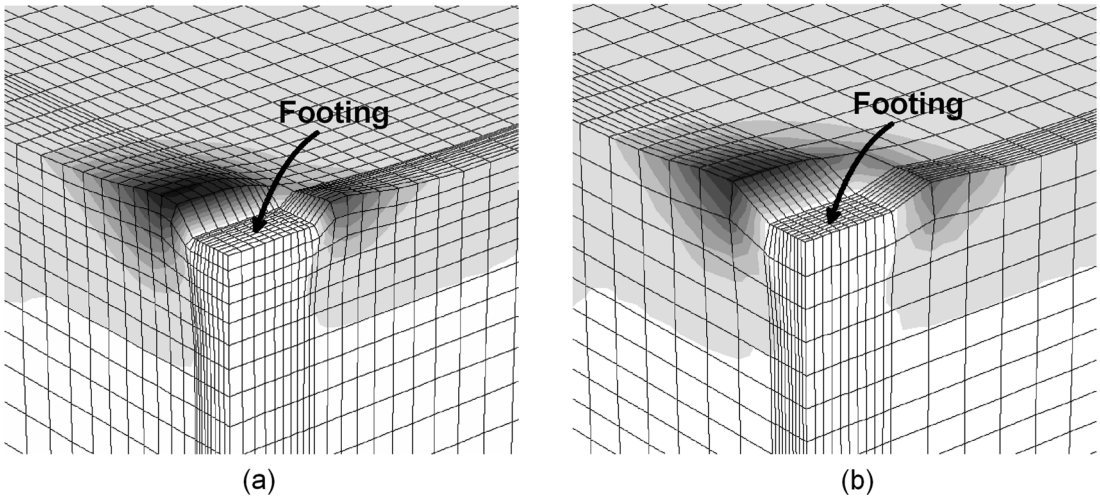

Fig. 1 (a) Distorted graded mesh for $L/B = 2$ and $\phi = 30°$ (displacement Magnification Factor = 3), and (b) bi-uniform mesh

modulus did not affect the bearing capacity calculated.

Two examples of a distorted mesh are illustrated in Fig. 1. One quarter of the footing indentation is presented on this figure for an aspect ratio of 2 and the internal friction angle of $\phi = 30^{o}$. To make the visualization clear, the displacements are magnified threefold.

Upon inducing geostatic stresses, uniform vertical downward velocities (displacement rates) were applied to the grid points within the footing plan (121 points); horizontal velocities were set to zero to model rough interface between the footing and the soil. The velocities were applied in several steps decreasing by the factor of 10. This procedure saved computational time while not affecting the final results, and it is recommended in running *FLAC3D* simulations (Michalowski and Dawson 2002a, 2002b, Erickson and Drescher 2002).

The bearing capacity was calculated as the ratio of the sum of vertical components of all forces acting on the footing to the footing area at the ultimate (steady-state) yielding. Analogous to Zhu and Michalowski's study, the footing area was extended to the mid-points of elements outside the footing plan. Once the modified bearing capacity factors N_{γ}^{*} were determined, the corresponding shape factors s_{γ} were calculated from Eq. (3), using N_{γ} obtained for the footing in the plane strain mode calculated by *FLAC3D*. These coefficients are presented in Table 1; for comparison, the slip-line solutions after Martin (2005), and the upper bound values after Michalowski (1997) are also presented in Table 1.

Table 1 Factor N_{γ} for strip footings

N_{γ}	Internal friction angle ϕ					
	15°	20°	25°	30°	35°	40°
FLAC3D	1.88	3.98	8.48	18.62	42.96	106.84
Slip-line Method (Martin 2005)	1.18	2.83	6.49	14.75	34.48	85.57
Upper Bound (Michalowski 1997)	1.93	4.46	9.76	21.39	48.68	118.82

Table 2 Shape factor s_{γ} from *FLAC3D* analysis

L/B	Internal friction angle ϕ					
	15°	20°	25°	30°	35°	40°
1	0.79	0.81	0.84	0.90	0.99	1.14
1.05	0.81	0.82	0.85	0.91	1.01	1.16
1.1	0.82	0.83	0.86	0.93	1.02	1.18
1.3	0.85	0.86	0.90	0.95	1.05	1.19
1.5	0.87	0.88	0.92	0.97	1.06	1.19
1.75	0.89	0.90	0.93	0.98	1.06	1.19
2	0.91	0.92	0.95	0.99	1.07	1.18
2.5	0.93	0.94	0.97	1.00	1.07	1.17
3.0	0.95	0.95	0.98	1.01	1.06	1.16
3.5	0.96	0.96	0.98	1.01	1.06	1.14
4	0.97	0.97	0.99	1.02	1.06	1.13

3. Computational results

Table 2 presents the computed shape factor s_γ as a function of internal friction angle ϕ and aspect ratio of the footing. For comparison, the results reported by Zhu and Michalowski (2005) are shown in Table 3. For smaller friction angle values, there is a very small difference between the results obtained from *FLAC3D* and from *ABAQUS*. The difference is small also for $\phi > 30^o$ and small aspect ratios (up to 2), but increases with an increase in the aspect ratio. This can be seen in Fig. 2 where the results are compared graphically. However, all differences are relatively small (note that s_γ-scale in Fig. 2 does not start at zero). These small differences can be attributed to algorithmic differences in the two codes, and the mesh size and element type used. Noticeably, *FLAC3D* simulations reproduce the existence of the peak in s_γ for higher ϕ values, albeit the peak becomes more pronounced for $\phi = 40^o$ rather than for $\phi = 35^o$ as reported by Zhu and Michalowski (2005). In general, the plausible argument of dilatancy playing an essential role put forward by Zhu and

Table 3 Shape factor s_γ after Zhu and Michalowski (2005)

L/B	Internal friction angle ϕ					
	15°	20°	25°	30°	35°	40°
1	0.80	0.81	0.85	0.93	1.02	1.17
1.5	0.87	0.88	0.91	0.99	1.06	1.17
2	0.90	0.91	0.94	1.00	1.05	1.16
3	0.93	0.95	0.97	1.01	1.03	1.10
5	0.95	0.97	0.98	1.00	1.01	1.07

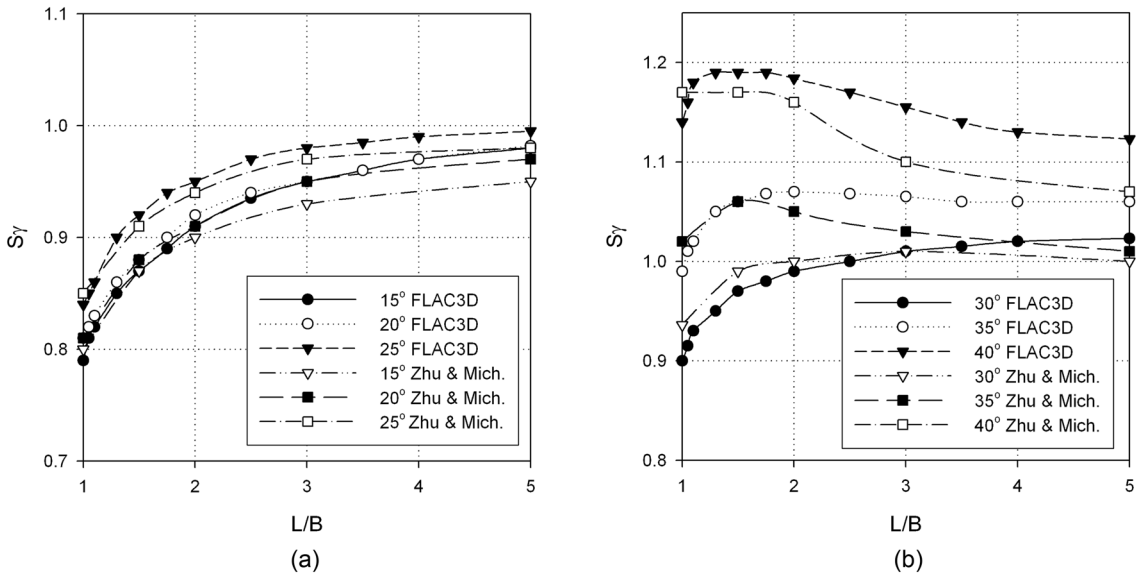

Fig. 2 Shape factor *versus* footing aspect ratio from the present solution and after Zhu and Michalowski (2005)

Table 4 Lower and upper estimates of shape factor s_γ after Lyamin *et al.* (2007)

L/B	Internal friction angle ϕ				
	25°	30°	35°	40°	45°
1	0.79*	0.86	0.96	1.06	1.18
	1.39**	1.48	1.71	2.16	2.92
1.2	0.73	0.78	0.83	0.84	0.83
	2.10	2.05	2.29	3.14	4.33
2	0.79	0.82	0.84	0.83	0.81
	1.92	1.87	2.08	2.73	3.71
3	0.80	0.82	0.82	0.79	0.75
	1.81	1.77	1.99	2.51	3.36
4	0.79	0.81	0.80	0.76	0.70
	1.74	1.71	1.96	2.38	3.16

*Lower estimate
**Upper estimate

Michalowski appears warranted.

It is interesting to notice that a similar effect is present in the results reported by Lyamin *et al.* (2007), who presented average lower/upper estimates of shape factors s_γ graphically, as function of B/L rather than L/B. They suggested a linear dependence of s_γ on B/L. A closer look at that dependence for $\phi = 35^o$ reveals a presence of a peak in s_γ. This peak is even more prominent in their upper estimates of s_γ shown in Table 4; clearly, a peak is present between $L/B = 1$ and $L/B = 2$ for every internal friction angle reported.

Zhu and Michalowski (2005) suggested the following analytic formulae to approximate the observed numerical trends in s_γ

$$s_\gamma = 1 + (0.6\tan^2\phi - 0.25)\frac{B}{L} \qquad \phi \le 30^o$$
$$s_\gamma = 1 + (1.3\tan^2\phi - 0.5)\left(\frac{L}{B}\right)^{1.5} e^{-\frac{L}{B}} \qquad \phi > 30^o \tag{4}$$

A rather minor modification for the results using *FLAC3D*, to fit the numerical outcome more accurately for case $\phi > 30^o$, can be made as follows

$$s_\gamma = 1 + (1.3\tan^2\phi - 0.5)\left(\frac{L}{B}\right)^{1.55} e^{-0.9\frac{L}{B}} \qquad \phi > 30^o \tag{5}$$

It is emphasized that the studies using *ABAQUS* and *FLAC3D* were independent. While the computational methodologies (algorithms) in the two codes are different, the results are nearly the same. This study confirmed the peculiarity found in s_γ, and it lends credibility to earlier results of Zhu and Michalowski (2005). While the differences between the two solutions are relatively small (up to about 2% for $\phi \le 25^o$, and up to about twice that for $\phi > 25^o$), the solution of Zhu and

Michalowski (2005) appears to yield slightly lower coefficients s_γ, and they might be preferred in design as they are more conservative.

4. Conclusions

The numerical values of the shape factor s_γ for square and rectangular footings obtained from *FLAC3D* simulations corroborate those obtained from *ABAQUS* simulations by Zhu and Michalowski (2005). For ϕ values of 35° and higher, *FLAC3D* confirms the existence of a peak in the s_γ function at some low aspect ratio L/B. Notwithstanding the inherent differences in the *FLAC3D* and *ABAQUS* codes and soil models used, the minor differences in s_γ demonstrate the overall equivalence of the results, and therefore the computational methods employed in the two codes.

Acknowledgements

The first two authors acknowledge support from the Shimizu Corporation, while the third author acknowledges the support from the National Science Foundation, Grant No. CMMI-0724022. The authors also thank Itasca Consulting Group for academic license of their *FLAC3D* code.

References

Bolton, M.D. and Lau, C.K. (1993), "Vertical bearing capacity factors for circular and strip footings on Mohr-Coulomb soil", *Can. Geotech. J.*, **30**(6), 1024-1033.

De Beer, E.E. (1970), "Experimental determination of the shape factors and the bearing capacity factors of sand", *Geotechnique*, **20**, 387-411.

Erickson, H.L. and Drescher, A. (2002), "Bearing capacity of circular footings", *J. Geotech. Geoenviron. Eng.*, **128**(1), 38-43.

FLAC3D (1997), "*Fast Lagrangian Analysis of Continua in 3 Dimensions*", Itasca Consulting Group, Minneapolis.

Golder, H.Q. (1941), "The ultimate bearing pressure of rectangular footings", *J. Inst.Civ. Eng.*, **17**(2), 161-174.

Hansen, J.B. (1970), "A revised and extended formula for bearing capacity", *Geoteknisk Inst., Bulletin* **28**, 5-11.

Lyamin, A.V., Salgado, R., Sloan, S.W. and Prezzi, M. (2007). "Two- and three-dimensional bearing capacity of footings in sand", *Geotechnique*, **57**(8), 647-662.

Martin, C.M. (2005), "Exact bearing capacity calculations using the method of characteristics", *Issues lecture, Proceedings of the 11th International Conference of IACMAG*, Turin, **4**, 441-450.

Meyerhof, G.G. (1963), "Some recent research on the bearing capacity of foundations", *Can. Geotech. J.*, **1**(1), 16-26.

Michalowski, R.L. (1997), "An estimate of the influence of soil weight on bearing capacity using limit analysis", *Soils Found.*, **37**(4), 57-64.

Michalowski, R.L. (2001), "Upper-bound load estimates on square and rectangular footings", *Geotechnique*, **51**(9), 787-798.

Michalowski, R.L. and Dawson, E.M. (2002a), "Three-dimensional analysis of limit loads on Mohr-Coulomb soil", *Foundations of Civil and Environmental Engineering* (FCEE), Poznan University of Technology **1**, 137-147.

Michalowski, R.L. and Dawson, E.M. (2002b), "Ultimate loads on square footings", *Proceedings of the 8th International Symposium on Numerical Models in Geomechanics (NUMOG V111)*, Rome, Balkema, Rottderdam, The Netherlands, 415-418.

Radenkovic, D. (1962), "Théorie des charges limites extension a la mécanique des sols", Séminaire de Plasticité. École Polytechnique, 1961, 129-141.

Zhu, M. and Michalowski, R.L. (2005), "Shape Factors for Limit Loads on Square and Rectangular Footings", *J. Geotech. Geoenviron. Eng.,* ASCE, **131**(2), 223-231.